Feasibility of Cold-Metal-Transfer Welding Magnesium AZ31 to Galvanized Mild Steel

Test results showed that zinc coating on the surface of the steel is critical to obtaining a sound CMT weld

BY R. CAO, J. Y. YU, J. H. CHEN, AND PEI-CHUNG WANG

ABSTRACT

Automotive manufacturers are faced with increasing pressure to reduce vehicle weight, improve fuel economy, reduce emissions, and enhance vehicle safety and performance. Therefore, an increasing number of vehicle structures are built using combinations of dissimilar materials such as steel, aluminum, and magnesium. Though the advantages are potentially huge, this hybrid fabrication approach raises substantial technical challenges to the design of vehicle structures and the associated joining processes. Differences in chemical and physical properties and the fact that neither solid solutions nor intermetallics exist between Mg and steel make the joining of Mg alloys to steels through conventional fusion welding impossible.

In this study, fusion welding of 1-mm-thick Mg AZ31 to 1-mm-thick galvanized mild steel lap joints was investigated. A cold metal transfer (CMT) fusion joining technique was adopted. Extensive welding tests with Mg wire were conducted and microstructures and element distributions were characterized. Based on the experimental results, it was found that CMT welding of Mg to steel is possible if the steel has a zinc coating because the zinc, which has a lower melting temperature than the steel, interacts with the molten Mg alloy to provide a braze joint. The brazing interface between the Mg weld metal and galvanized mild steel primarily consists of Al, Zn, and Mg intermetallics and solid solution, such as Mg solid solutions, $MgFeAlO_4$, Fe_2O_3, and Mg_2Zn_{11}. The strength of the CMT weld-brazed, lap-shear, 1-mm-thick Mg AZ31-galvanized mild steel joint is comparable to the strength of a lap-shear 1-mm-thick Mg AZ31-Mg AZ31 welded joint.

Introduction

Automotive manufacturers are faced with increasing pressure to reduce vehicle weight, improve fuel economy, reduce emissions, and enhance vehicle safety and performance. Therefore, an increasing number of vehicle structures are built using joints of dissimilar materials such as steel, aluminum, and magnesium. Although the advantages in mass savings are potentially huge, this hybrid fabrication approach raises substantial technical challenges to the design of vehicle structures and the associated joining processes. Conventional fusion welding of magnesium alloys to steels produces joints with brittle MgO particles that degrade the joint strength significantly (Ref. 1).

Cold metal transfer (CMT) technology for joining similar and dissimilar materials has been developed by Fronius International (Ref. 2). The method has been shown to be a feasible alternative to adhesive bonding and mechanical fastening for joining dissimilar materials, e.g., particularly for aluminum to galvanized steel (Ref. 3). The key feature of this process is that the motion of the wire has been integrated into the joining process and into the overall control of the process. The wire retraction motion assists droplet detachment during the short circuit, thus the metal can transfer into the welding pool without the aid of the electromagnetic force. Then the heat input and spatter can be controlled. As a result, the heat input can be properly controlled and , consequently, sound joints can be produced.

While a great deal of effort has been focused on CMT joining of aluminum alloy to steels (Refs. 4–6), there is a need to join magnesium to steel (Refs. 7–9). Magnesium alloys have been widely used in the automotive industry for their low density, high strength-to-weight ratio, good castability, and being easily recycled (Refs. 10–12). However, there are specific challenges to joining magnesium to steel. The maximum solid solubility of Fe in Mg is 0.00043 at.-%, and that of Mg in Fe is nil (Refs. 13, 14). The melting points of Mg and Fe are 649° and 1539°C, respectively. This huge difference in melting points makes it difficult to melt both metals in a welding pool required for a fusion welding process. Moreover, both metals are immiscible in a liquid state due to density differences, and they do not react to form any congruent molten phase(s). Therefore, it is extremely difficult to join magnesium alloys to steels through conventional fusion welding.

Recently, Liu et al. (Ref. 1) made a joint of Mg AZ31B alloy to 304 steel in a lap configuration with AZ31B on the top by a hybrid laser-gas tungsten arc welding (GTAW) technique. Their results indicated the weld fractured at the Mg-Fe interface with a poor joint strength. The authors attributed such low mechanical strength to the severe oxidation at the Mg/Fe interface. In later work, Liu et al. (Refs. 15, 16) joined the magnesium alloy and steel by hybrid laser-GTA welding with Ni foil as an interlayer. With the addition of a Ni interlayer in a lap joint configuration, AZ31B Mg alloy and mild steel were successfully joined using a hybrid laser/GTA welding process. The joint is produced by the formation of two intermediate phases between Mg and Ni, and the solid solution of Ni in Fe. The strength of the joints reached approximately 176 MPa, i.e., 110% that of the base Mg alloy, which has a strength of 160 MPa (Ref. 15). The addition of a Ni interlayer altered the bonding mode of the magnesium alloy to steel joint from a mechanical interlock without metallurgical reactions to that of semimetallurgical bonds, which improved

R. CAO, J. Y. YU, and J. H. CHEN are with Lanzhou University of Technology, Lanzhou, Gansu, China. PEI-CHUNG WANG is with the General Motors Manufacturing Systems Research Lab, Warren, Mich.

KEYWORDS

Magnesium AZ31
Mild Steel
Cold Metal Transfer (CMT)
Weld-Braze Process

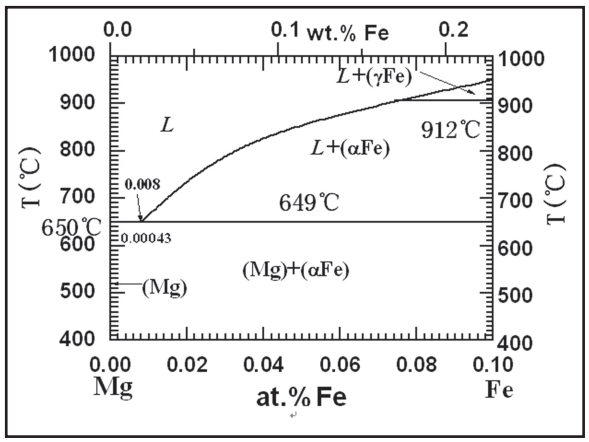

Fig. 1 — Phase diagram of Mg-Fe (Ref. 13).

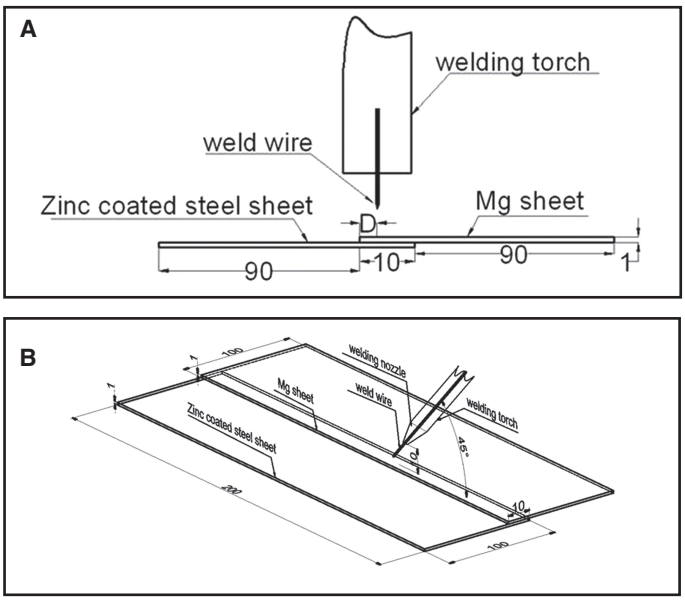

Fig. 2 — Schematic of lapped magnesium-to-steel sheet: A — Plane view; B — side view of the welding torch with respect to the sample (dimensions in mm).

the joint strength in the interlayer fusion welding process. However, the addition of an interlayer adds additional cost and cycle time and so an alternative route to a fusion joint is required.

Other than fusion welding, a few studies in friction stir welding (FSW) indicated the ability to join magnesium alloys to steel (Refs. 17–20). Watanabe et al. (Ref. 17) first studied the feasibility of joining a magnesium alloy to steel in a butt-joint configuration. Maximum joint strength was noted to be 70% of the strength of the magnesium base metal. Chen and Nakata (Ref. 18) studied the effect of tool geometry on the microstructure and mechanical properties of a friction stir lap-welded Mg alloy and steel joint. S. Jana (Ref. 19) has studied FSW of a Mg alloy to steel in a lap configuration. A friction stir weld that could achieve 80% of the base metal strength was fabricated. Joints were found to be mechanical in nature since the Mg/steel bonded interface directly under the tool tip was mostly free from any new Zn-Mg phase. The top Zn coating melted as a result of the process heat and subsequently dissolved the magnesium from the top sheet to form Zn-Mg liquid alloy. The thin Zn coating could not act as a brazing alloy.

The purpose of the current study is to investigate the feasibility of using the CMT welding process to join Mg AZ31 to mild steel. There are three main parts in this paper. The first presents the experimental procedure, including material, sample fabrication, microstructural observation and analysis, mechanical testing, and fracture analysis. The next section presents the results and discusses the feasibility of CMT joining magnesium to steel and optimization of welding variables. Finally, we discuss microstructure of optimized welded joints and bonding mechanism of the welded Mg AZ31 to galvanized mild steel joints.

Experimental Procedure

Materials

One-mm-thick Mg AZ31B alloy sheet with a nominal composition of Mg-3Al-1Zn-0.2Mn-0.1Si (wt-%), and 1-mm-thick hot-dipped galvanized mild carbon steel sheets with nominal composition of Fe-0.01C-0.01Si-0.39Mn-0.03P-0.025S (wt-%) were used in this study. The thickness of the Zn coating was 8.5 μm. Al 4043 wire with a diameter of 1.2 mm and AZ61Mg wire with a diameter of 1.6 mm were used. Per the manufacturer's datasheet, Table 1 lists the wire compositions.

Joining Strategy

Figure 1 is the Mg-rich portion of the Mg-Fe phase diagram having a maximum solid solubility of 0.00043 at.-% Fe in Mg. Neither solid solutions nor intermetallics form. Furthermore, the melting points of the Mg and Fe are 649° and 1539°C, respectively. This huge difference in melting points makes it very difficult to melt both in a welding pool. Therefore, in this study a welding-brazing process is proposed to join the Mg AZ31 to mild steel in a lap joint configuration. During the joining process, while welding occurs between the melting Mg AZ31 base metal and molten wire, brazing develops between the molten wire and zinc coating on the surface of the steel. As a result, a weld-braze joint is formed for Mg AZ31 to galvanized mild steel. To achieve this welding-brazing process, cold metal transfer (CMT) joining technology was adopted.

Sample Fabrication

The lap-shear joint configuration, shown in Fig. 2, was selected for this study. The joints were fabricated from 200 mm × 50 mm × 1 mm sheets. A fillet weld was located on one edge of a 10-mm overlap region. A fixture was used to ensure consistent weld placement. Prior to welding, the Mg AZ31 sheets were degreased with acetone then polished with an abrasive cloth. The mild steel sheets were only degreased with acetone. As shown in Fig. 2, the Mg AZ31 sheet was placed on the top of the steel in a lap configuration with an overlap distance of 10 mm. The deviated distance (D) is defined as the deviation from the welding torch to the edge of the lapped weld joint. If the steel is placed on the top of the Mg

Table 1 — Chemical Compositions of Wires (wt-%)

Wires	Si	Fe	Cu	Mn	Zn	Ti	Be	Ce	Ni	Mg	Al	Other
Al4043	4.5~6.0	0.80	0.30	0.05	0.10	0.20				0.05	Bal.	
MgAZ61	≤0.05	≤0.005	≤0.05	0.15–0.5	0.4–1.5		0.0006		≤0.005	Bal.	5.8–7.2	0.3

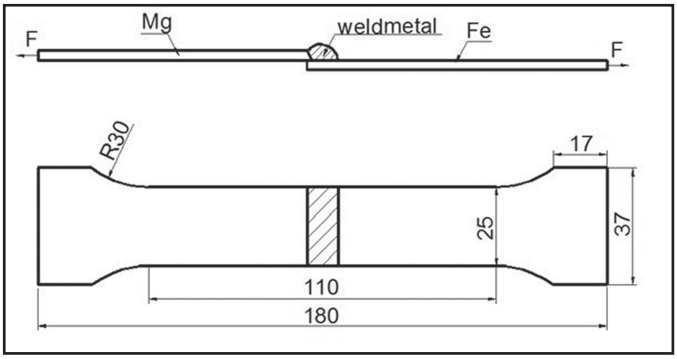

Fig. 3 — Specimens machined from CMT welded Mg-steel sheets (dimensions in mm).

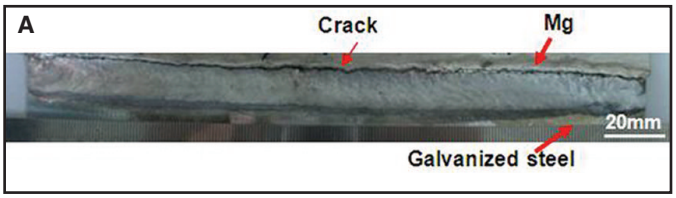

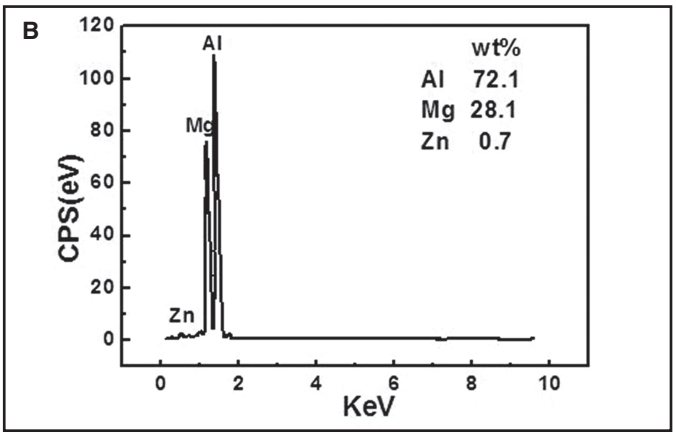

Fig. 4 — A — Appearance of CMT welded magnesium AZ31 to galvanized mild steel with wire Al4043; B — EDS elements analysis results of cracking locations shown in Fig. 4A.

AZ31 sheet, most of the Mg element in the Mg AZ31 alloy would have been vaporized as the mild steel becomes molten and a sound weld could not be formed. The angle between the welding torch and lap joint was 45 deg from the normal to the sheet metal in the direction of the weld — Fig. 2B. The welding direction is parallel to the lapped joint. In this arrangement, while the top Mg AZ31 becomes molten, the mild steel underneath would remain unmelted. The molten magnesium AZ31 spreads and contacts the galvanized steel and, as a result, a weld-braze joint is formed.

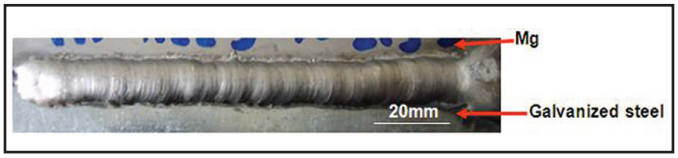

Fig. 5 — Appearance of the CMT weld of magnesium AZ31 to galvanized mild steel using welding wire Mg AZ61.

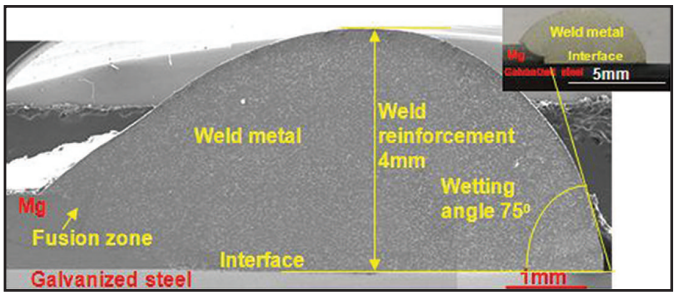

Fig. 6 — Cross section of the welded Mg AZ31 to galvanized mild steel joints.

Orthogonal Experimental Design

The Taguchi DOE technique (Ref. 21) incorporating orthogonal arrays was utilized for the systematic evaluation of the welding variables. Table 2 shows the orthogonal array corresponding to five factors and four levels. L_{32} with the subscript 32 denotes the number of experiments to be performed. The L_{32} orthogonal array has been shown in Table 3. Each column in Table 3 represents a test parameter whereas each row represents a test condition that is formed by a combination of different levels of the investigated parameters.

The design of orthogonal experiments can greatly reduce the time and increases the accuracy of assigning proper columns for interaction effects (Ref. 21). In the current design, wire feed speed (parameter A) has been assigned to the 1st column, and weld speed (parameter B) to 2nd column. The interaction factor between parameters A and B is assigned to the 3rd column. Factor C (deviation distance) was assigned to the 4th column and interaction between factors A and C (A × C) to column 5, and factor D, voltage, and E, Zn coating thickness, to column numbers 6 and 8, respectively. Based on the output response, the tensile load, in all the 32 investigated cases, Taguchi experimental design was analyzed using Matlab software (Ref. 22).

Table 2 — Experimental Factors and Levels

Control Factors	Levels				Units
	I	II	III	IV	
Wire feed speed (A)	3	4	5	7	m/min
Welding speed (B)	7	8	9	10	mm
Deviation distance (C)	0	1	2	4	mm
Voltage (D)	10	14	18	22	Volt
Thickness of zinc coating (E)	4	5.3	11.6	6	μm

Analytical Analysis

The metallographic cross sections of the specimens were prepared and examined. The ground and polished specimens were etched using 5 g picric + 10 mm distilled water + 50 mL ethanol + 5 g acetic acid for Mg AZ31 and by Nital (4 vol-% HNO_3 + 96 vol-% ethanol) for the mild steel. The microstructures of the weld were observed by scanning electron microscope (SEM 6700F) equipped with an energy-dispersive X-ray spectrometer (EDS). The analyses of element distributions of the welds were carried out by electron probe microanalysis (EPMA).

Mechanical Testing

The specimens shown in Fig. 3 were machined from the weldment. Quasi-static tests were performed by loading each specimen to failure in a tensile tester to minimize bending stresses inherent in the testing of lap shear specimens, filler plates were attached to both ends of the sample using masking tape to accommo-

date the sample offset. Load vs. displacement curves were obtained as the specimens were loaded at a stroke rate of 1 mm/min. Three to four replicates were performed, and the average peak loads were reported.

Fracture Analysis

The fracture location and fracture surface was analyzed by scanning electron microscope (SEM 6700F).

Results and Discussion

Feasibility of CMT Joining Mg AZ31 to Mild Steel

To determine the proper welding wire, the Fe-Mg phase diagram, shown in Fig. 1, was reviewed for potential stable room-temperature compounds. As indicated in Fig. 1, because neither solid solutions nor intermetallics form between iron and magnesium, a wire should include elements that have significant solid solubility for magnesium. According to Ref. 14, the solid solubility of Mg in aluminum reaches a peak value of 11.8 at.-%. Furthermore, the Al element would react with the Mg as well as iron. Therefore, feasibility tests of CMT welding of Mg AZ31 to galvanized mild steel with commercially available Al4043 wire were performed.

Magnesium-steel CMT tests by Al 4043 wire were performed with the process variables shown in Table 4. Figure 4A shows the welded Mg AZ31 to galvanized mild steel. As shown, significant cracks were observed in the weld metal for both cases even though a large solid solubility exists between Al and Fe, and Al and Mg. Figure 4B shows EDS analysis result on the regions where cracks are produced in the welds. Results have presented that the cracks are caused by a significant

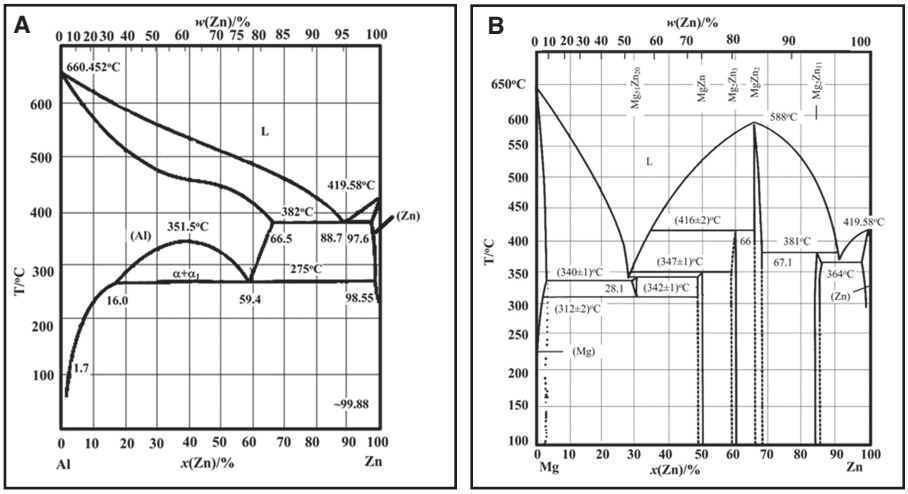

Fig. 7 — Phase diagrams of the following: A — Al-Zn (Ref. 14); B — Mg-Zn (Ref. 13).

Table 3 — Input Parameters of Orthogonal Array

Column Number	1	2	3	4	5	6	7	8	9
Exp.	A	B	A×B	C	A×C	D	C×D	E	
1	3	7	1	0	1	10	1	4	1
2	3	8	2	1	2	14	2	5.3	2
3	3	9	3	2	3	18	3	11.6	3
4	3	10	4	4	4	22	4	6	4
5	4	7	1	1	2	18	3	6	4
6	4	8	2	0	1	22	4	11.6	3
7	4	9	3	4	4	10	1	5.3	2
8	4	10	4	2	3	14	2	4	1
9	5	7	2	2	4	10	2	11.6	4
10	5	8	1	4	3	14	1	6	3
11	5	9	4	0	2	18	4	4	2
12	5	10	3	1	1	22	3	5.3	1
13	7	7	2	4	3	18	4	5.3	1
14	7	8	1	2	4	22	3	4	2
15	7	9	4	1	1	10	2	6	3
16	7	10	3	0	2	14	1	11.6	4
17	3	7	4	0	4	14	3	5.3	3
18	3	8	3	1	3	10	4	4	4
19	3	9	2	2	2	22	1	6	1
20	3	10	1	4	1	18	2	11.6	2
21	4	7	4	1	3	22	1	11.6	2
22	4	8	3	0	4	18	2	6	1
23	4	9	2	4	1	14	3	4	4
24	4	10	1	2	2	10	4	5.3	3
25	5	7	3	2	1	14	4	6	2
26	5	8	4	4	2	10	3	11.6	1
27	5	9	1	0	3	22	2	5.3	4
28	5	10	2	1	4	18	1	4	3
29	7	7	3	4	2	22	2	4	3
30	7	8	4	2	1	18	1	5.3	4
31	7	9	1	1	4	14	4	11.6	1
32	7	10	2	0	3	10	3	6	2

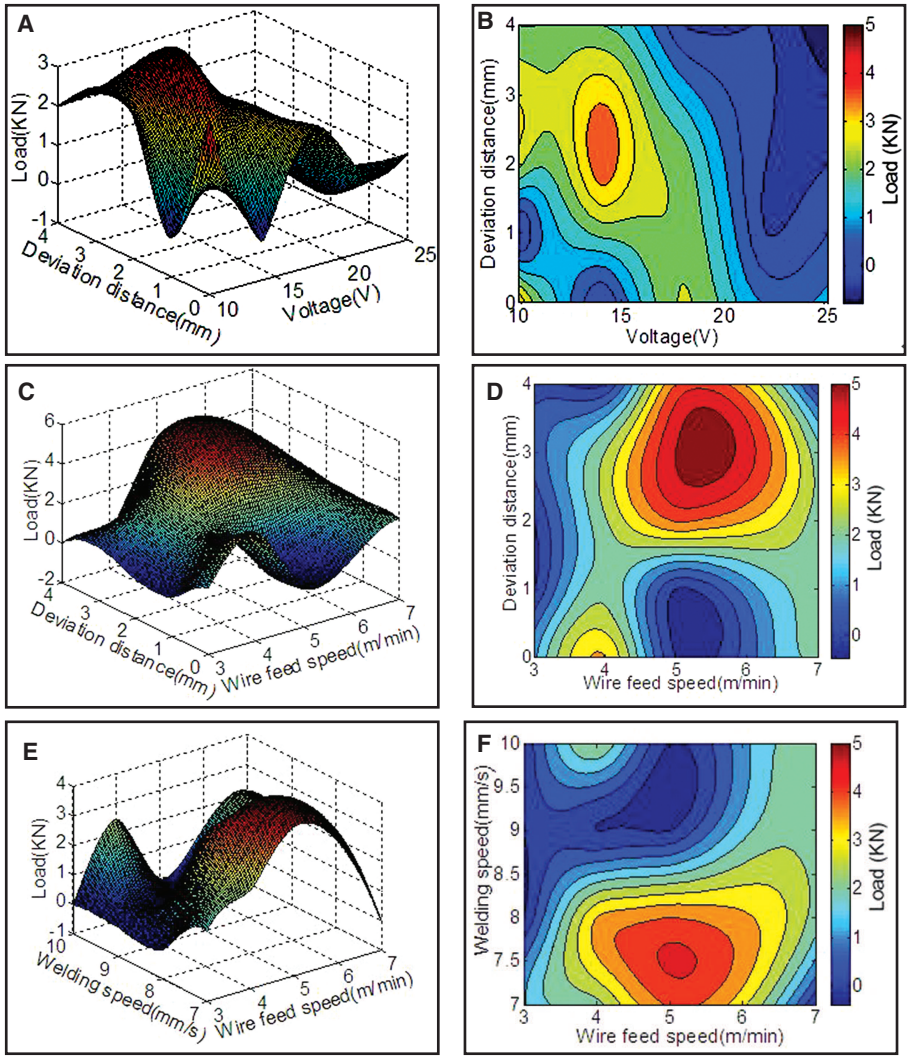

Fig. 8 — Combined effects of the following: A, B — Welding voltage and deviation distance; C, D — wire feed speed and deviation distance; E, F — wire feed speed and welding speed on the strength of a Mg AZ31 to mild steel weld joint.

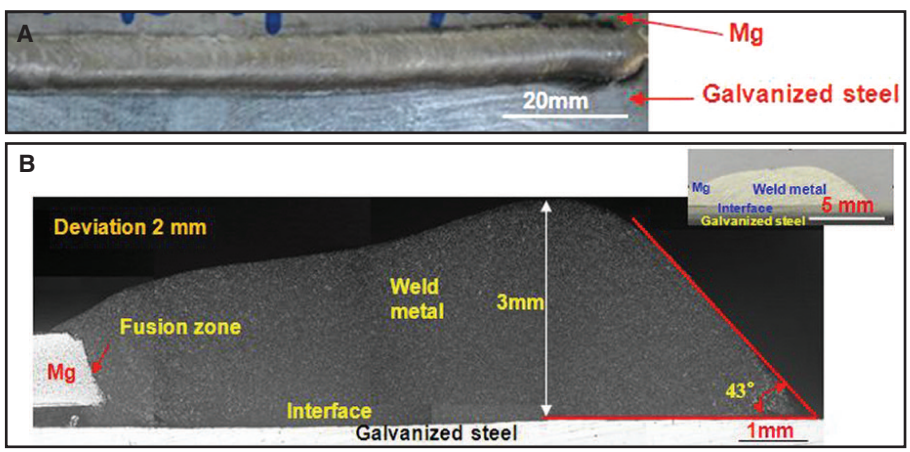

Fig. 9 — A — Appearance; B — cross sections of optimized CMT welded Mg AZ31-galvanized mild steel joints.

amount of intermetallic compound Mg_2Al_3 between the Al6061-T6 and Mg AZ31. As a result, it is not feasible to join Mg AZ31 to galvanized mild steels with welding wire Al4043.

As described in Refs. 23–25, sound joints between the Mg wire and Mg alloy base metal can be produced using gas metal arc welding (GMAW). In our tests, Mg AZ61 wire was selected next in our experimental trials.

Welding tests were conducted, and Table 5 lists the process variables. Figure 5 shows the appearance of the Mg AZ31 to galvanized mild steel weld. For the Mg AZ31 to galvanized mild steel welded joint, the sound weld, shown in Fig. 5, composed of the weld metal, fusion zone on the Mg sheet and the brazing interface between the weld metal and nonmelted galvanized mild steel sheet was obtained. Examination of the cross section shown in Fig. 6 showed that although sound bonds formed between magnesium and steel, a large wetting angle of about 70 deg and a high weld reinforcement of 4 mm were observed on the steel surface, which indicates that the wetting of the molten droplet on the steel substrate is poor. Poor wetting would constrain the brazing area between the magnesium and steel. Since the strength of the Mg-steel joints is closely related to the brazing area of the molten droplet on the steel, poor wetting (i.e., large wetting angle) would lead to poor joint strength. Thus, further study to improve the CMT joining of Mg AZ31-galvanized mild steel is needed.

Improvement of CMT Joining of Mg to Steel

To improve the wetting of the molten Mg AZ61 wire on the zinc-coated steel, we examined the phase diagrams of Al-Zn and Mg-Zn (Ref. 14) shown in Fig. 7A and B, respectively. Because the solid solubility of Zn in Al is high (66.5% at 382°C) and Zn in Mg is relatively low (3% at 325°C), the potential exists for the brazing interface to be produced by forming the Al and Zn solid solution and thereby improving the wetting angle.

Experimental results of the Al-steel welding-brazing process showed the presence of the zinc coating improves the wetting angle (Refs. 26, 27). In our work, it was necessary to limit the arc heat input to avoid vaporization of the zinc coating by using Mg wire that contained Al content. To achieve this, the welding torch, shown in Fig. 2, was positioned at a sufficient distance from the lap joint so that molten magnesium was in contact with the zinc-coated steel during welding, and consequently the zinc coating could react with the Al and Mg in the welding wire yet not vaporize. As a result, the solubility and wettability of weld metal on the zinc-coated steel would be improved. In the following sections, process optimization, microstructure, bonding mechanism, effect of the torch location on the weld appearance, fracture location, and strength of the Mg to galvanized steel joints are discussed.

Optimization of the Welding Variables

To optimize the welding variables, a quadratic regression analysis of various variables was performed. Table 6 presents the process parameters of orthogonal

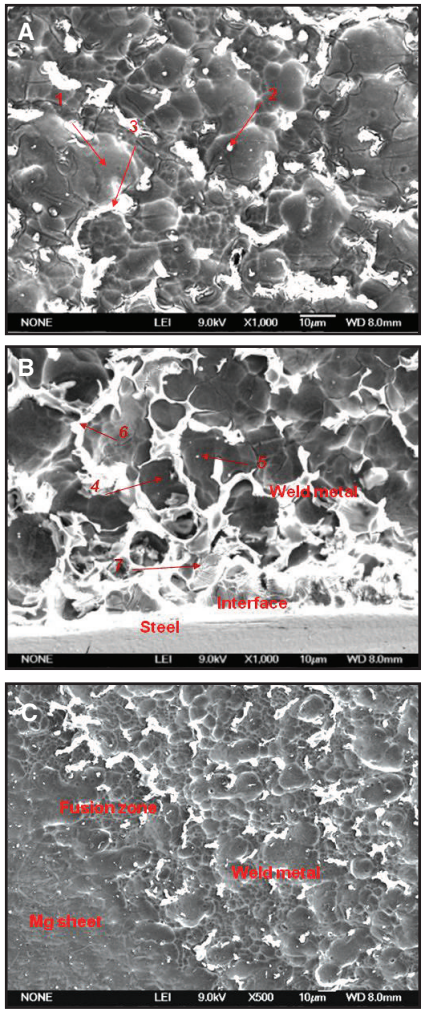

Fig. 10 — Cross-section microstructure of CMT welded Mg AZ31 to mild steel joints at the following: A — Middle of the weld metal; B — weld metal near the brazing interface; C — fusion zone.

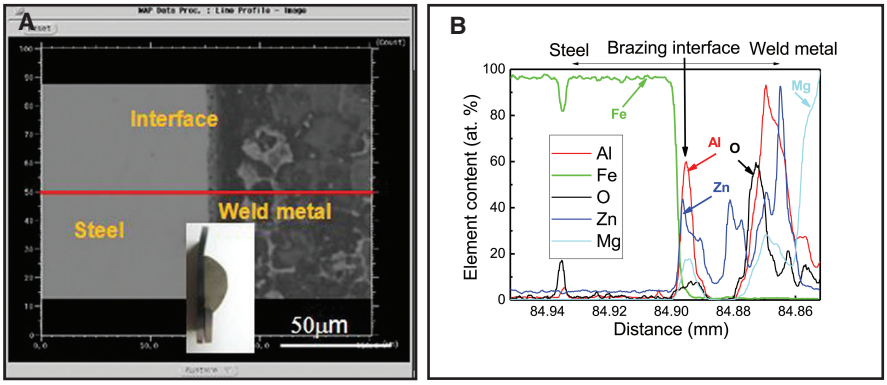

Fig. 11 — Results of line analysis across the interface of Mg AZ31 to galvanized mild steel joint fabricated with optimized welding parameters: A — Cross section; B — element distribution along the red line in Fig. 11A.

Table 4 — Process Variables for CMT Welded Mg AZ31 to Galvanized Mild Steels with Al4043 Wire

Material	Wire Diameter (mm)	Wire Feed Speed (m/min)	Current (Amp)	Voltage (Volt)	Welding Speed (mm/s)
Mg AZ31 to galvanized mild steel	1.2	3	45	12	4.17

array and the characteristics. The peak load to fracture of the joints (i.e., joint strength) was the metric used as the basis for the process optimization.

Table 7 shows the analysis results on the rank of the process parameters using the Taguchi method. As shown in Table 7, the 'delta' value was estimated for each parameter from the difference of the maximum and minimum mean tensile load values at different levels. The rank of each parameter generated by the Taguchi method was determined from the delta values of all the parameters. The rank of the parameters signifies their relative importance in terms of their influence on the output response, i.e., tensile peak loads in this investigation. As shown in Table 7, the variables in the order of importance are as follows: wire feed speed (A) > welding speed (B) > thickness of zinc coating (E) > the interaction effects of wire feed speed and welding speed (A × B) > welding voltage (D) > deviation distance (C) > the interaction effects of wire feed speed and deviation distance (A × C) > the interaction effects of deviation distance and welding voltage (C × D). When a single factor is considered, optimized welding variables can be obtained, i.e., a wire feed speed of 4 m/min, a weld speed of 7 mm/s, and a voltage of 18 V.

A statistical analysis of variance (ANOVA) was performed to determine the statistical significance of the process parameters (Ref. 28). It helps to determine the effect of an individual input parameter on the output parameters. Table 8 shows the results of the ANOVA analysis. Based on these results, the coating thickness was found to be the most influential process parameter with a 20.45% contribution followed by welding voltage (17.33%), weld speed (16.7%), and wire feed speed (15.14%). The combined main effects of various process variables on the joint strengths pertaining to the ANOVA analyses are shown in Fig. 8. From Fig. 8, the red region indicates the maximum load, so the optimized welding window (i.e., welding voltages of 14 to 16 V, deviation distances of 2 to 3.5 mm, welding speeds of 7 to 8 mm/s, and wire feed speeds of 4.5 to 6 m/min) were developed by combining the results shown in Fig. 8 and Table 6.

Weld Appearance of Optimized Mg AZ31-Mild Steel Joint

Cold metal transfer welding of Mg AZ31 to galvanized mild steel was performed with the optimized welding variables shown in Table 9. The weld appearance and cross sections of the optimized Mg AZ31-galvanized mild steel welded joints are presented in Fig. 9. As shown in Fig. 9, a sound weld was composed of the weld metal, fusion zone on the Mg AZ31 sheet, and the brazing interface between the weld metal and nonmelted galvanized mild steel. Examination of the cross section showed the wetting angle and weld reinforcement were improved compared with the nonoptimized results shown in Fig. 6.

Microstructure of Optimized Mg AZ31-Mild Steel Joints

To understand the material properties of CMT welded Mg AZ31 to galvanized mild steel with magnesium AZ61 welding wire, the weld microstructures were analyzed. Figure 10 and Table 10 present the detailed microstructures and detailed EPMA analyses of three regions (i.e., weld metal center, weld metal near the brazing interface, and fusion zone) shown in Fig. 9B. Since Region 1 in Fig. 10A contains 93 at.-% Mg and a small amount of O and Zn, the phase in Region 1 is α-Mg solid solution. Region 2 in Fig. 10A contains 65.23 at.-% O, 25.81 at.-% Mg, and a small amount of Al and Zn, and, consequently, the corresponding phase is likely an oxide inclusion. For Region 3, it contains 54.38 at.-% Mg and 36.22 at.-% Al, which is consistent with the β-$Al_{12}Mg_{17}$ intermetallic. Based on these analyses, the microstructure at the center of the weld metal is composed of an α-Mg solid-solution dendritic structure (denoted by Region 1), which contains a few oxide inclusions (refer to Region 2), with the eutectic structure along the grain boundaries consisting of β-$Al_{12}Mg_{17}$ mesh intermetallic (denoted by region 3). The microstructure of the weld metal near the combined interfaces is composed of α-Mg solid solution (denoted by Region 4 in Fig. 10B), a

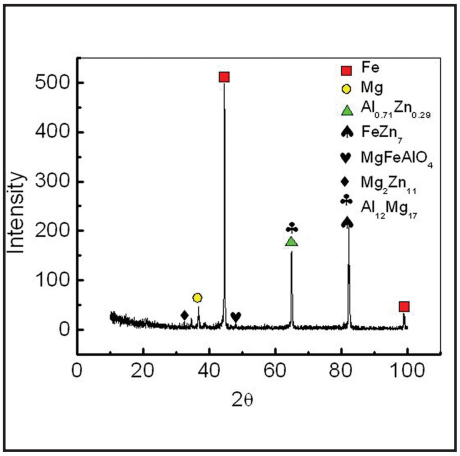

Fig. 12 — X-ray analysis at the brazed Zn-coated mild steel/weld metal (with Mg AZ61 welding wire) interface.

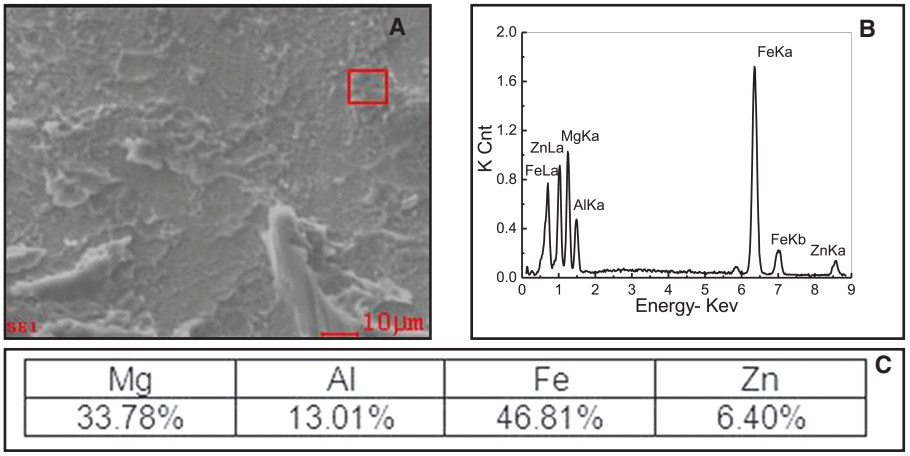

C

Mg	Al	Fe	Zn
33.78%	13.01%	46.81%	6.40%

Fig. 13 — A — Fractography of a tested specimen; B — distribution of the element; C — element analysis of a square region shown in A.

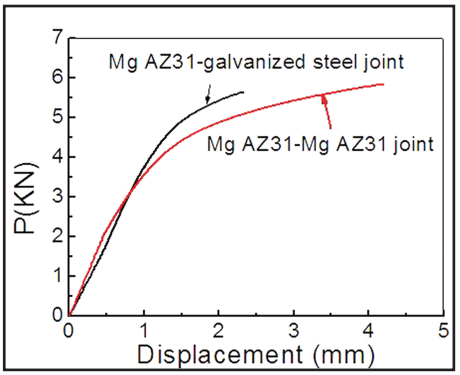

Fig. 14 — Load-displacement of lap-shear tests of CMT joined Mg AZ31-galvanized steel and Mg AZ31-Mg AZ31 specimens.

few oxide inclusions (denoted by Region 5), and coarse β-$Al_{12}Mg_{17}$ eutectic (denoted by Region 6) and MgZn intermetallic compounds (denoted by Region 7 in Fig. 10B). The fusion zone that is formed by weak metallurgical reactions between the magnesium alloy and the weld metal is narrow and the grains are small due to a relatively higher cooling rate as a result of the steel substrate acting as a heat sink.

Bond Mechanism of Mg-Steel Joints

As described in Refs. 1, 15, and 16, the strength of dissimilar Mg-steel joints is mainly determined by the brazing interface between the melted Mg weld metal and nonmelted galvanized steel sheets. To understand the bond mechanism at the brazing interface, EPMA was employed to analyze the brazing interface of the welded Mg AZ31-galvanized mild steel joints. Figure 11A, B shows the cross section of a weld and the line analysis results for an optimized joint, respectively. As shown in Fig. 11A, the bright image on the left-hand side is the steel and the weld metal on the right-hand side, and the gray zone between the steel and weld metal is the brazed interface. EPMA line analysis results shown in Fig. 11B indicate the narrow interface zone is composed of Al, Zn, and Mg elements. The Al and Zn content is higher than the Mg content in the brazing interface although the Mg Alloy AZ61 was used as the welding wire. Thus, the brazed zone between the weld metal and steel sheet was formed by a combination of Al, Zn, and Mg. Because the Al content at the interface was greater than the Mg content, we conclude that the Al alloying element within the AZ61 wire and Mg sheet in combination with the Zn content from the coating play an important role for enhancing the wettability of the Mg on Fe. The line analysis results in Fig. 11B also highlights the eutectic β-$Al_{12}Mg_{17}$ within the weld metal on the right-hand side of the picture.

In order to confirm the bonding mechanism of the brazed joints, X-ray analyses of the interface of the specimens fractured along the interface between the weld metal and Zn-coated steel were conducted, and the results are presented in Fig. 12. It was found that the interface is mainly composed of the Mg-Al eutectic structure and various intermetallics — $MgFeAlO_4$, Fe_2O_3, and Mg_2Zn_{11}.

Examination of the bonding mechanism for the joints made with the weld torch deviated by 1 mm was also performed, and the results are presented in Fig. 13. The fractured interface of a specimen shown in Fig. 13A indicates a shear tear fracture feature. Similar fracture features were observed for the joints without the torch deviation. Figure 13B shows the element content of marked red regions shown in Fig. 13A. Figure 13C shows the element distributions. It was found that there is a significant amount of Al and Zn elements in addition to the Mg and Fe elements observed on the fracture surface. All these results imply that Al and Zn elements can improve the wettability of the brazing interface. Aluminum plays an important role in improving the wettability of a Mg-rich weld metal on Zn-coated steel sheet. The effect of Al on the formation of the Mg AZ31-galvanized mild steel brazing joint needs to be studied further.

Strength of Mg-Steel Joints

Static testing of optimized CMT welding-brazing Mg AZ31-galvanized steel joints was performed, and the results are presented in Fig. 14. For the purposes of the comparison, test results of CMT welding-brazing Mg AZ31-Mg AZ31 joint with the same dimensions were also included in Fig. 14. For the sake of clarity, only one representative result was presented. As shown, CMT welding-brazing Mg AZ31 galvanized mild steel joint has a comparable strength to CMT welding-brazing Mg AZ31-Mg AZ31 joint.

Table 5 — Process Variables for CMT Welded Mg AZ31 to Galvanized Mild Steel with AZ61 Magnesium Wire

Material	Wire Diameter (mm)	Wire Feed Speed (m/min)	Current (Amp)	Voltage (Volt)	Welding Speed (mm/s)
Mg AZ31 to galvanized mild steel	1.6	3	50	10	5.5

Table 6 — Input Parameters of Orthogonal Array and the Output Characteristics

Column Number	1	2	3	4	5	6	7	8	9	Joint Strength
Exp	A	B	A×B	C	A×C	D	C×D	E		(kN)
1	3	7	1	0	1	10	1	4	1	2.8
2	3	8	2	1	2	14	2	5.3	2	0
3	3	9	3	2	3	18	3	11.6	3	0
4	3	10	4	4	4	22	4	6	4	0
5	4	7	1	1	2	18	3	6	4	4.7
6	4	8	2	0	1	22	4	11.6	3	1.9
7	4	9	3	4	4	10	1	5.3	2	0
8	4	10	4	2	3	14	2	4	1	4.4
9	5	7	2	2	4	10	2	11.6	4	4.8
10	5	8	1	4	3	14	1	6	3	4.0
11	5	9	4	0	2	18	4	4	2	0
12	5	10	3	1	1	22	3	5.3	1	0
13	7	7	2	4	3	18	4	5.3	1	0
14	7	8	1	2	4	22	3	4	2	0
15	7	9	4	1	1	10	2	6	3	0
16	7	10	3	0	2	14	1	11.6	4	0
17	3	7	4	0	4	14	3	5.3	3	0
18	3	8	3	1	3	10	4	4	4	0
19	3	9	2	2	2	22	1	6	1	0
20	3	10	1	4	1	18	2	11.6	2	0
21	4	7	4	1	3	22	1	11.6	2	0
22	4	8	3	0	4	18	2	6	1	5.1
23	4	9	2	4	1	14	3	4	4	0
24	4	10	1	2	2	10	4	5.3	3	0.5
25	5	7	3	2	1	14	4	6	2	3.3
26	5	8	4	4	2	10	3	11.6	1	4.0
27	5	9	1	0	3	22	2	5.3	4	0
28	5	10	2	1	4	18	1	4	3	0
29	7	7	3	4	2	22	2	4	3	0
30	7	8	4	2	1	18	1	5.3	4	4.5
31	7	9	1	1	4	14	4	11.6	1	4.3
32	7	10	2	0	3	10	3	6	2	4.2

Table 7 — Ranking of Influential Process Parameters by Taguchi Method

Corresponding No.	A	B	A×B	C	A×C	D	C×D	E
Delta	6.6	4.1	3.4	2.4	1.3	3.1	1.1	4
Rank	1	2	4	6	7	5	8	3

A: wire feeder speed, B: welding speed, C: deviation distance, D: welding voltage, E: thickness of zinc coating

Conclusions

The present study provides a feasible fusion method for joining of magnesium AZ31 to hot dipped galvanized mild steel for automotive applications. Extensive tests conducted on the CMT welding of 1-mm-thick lap-shear Mg AZ31 sheet to 1-mm-thick mild steel sheet concluded the following:

1. Cold metal transfer (CMT) welding of 1-mm-thick lap-shear Mg AZ31 sheet to 1-mm-thick galvanized mild steel sheet with welding wire Mg AZ61 has been developed. Test results showed that zinc coating on the surface of the steel is critical to obtaining a sound CMT welded Mg AZ31 to coated mild steel joint.

2. Cold metal transfer welded Mg AZ31 to galvanized mild steel joints were composed of the fusion zone of the Mg AZ31 sheet and Mg AZ61 welding wire, the Mg weld metal, i.e., combined welding wire and Zn coating, and the brazing interface between the Mg weld metal and galvanized mild steel sheet. The brazing interface consists of Al, Zn, Mg intermetallic compounds and oxides (i.e., $MgFeAlO_4$, Fe_2O_3, and Mg_2Zn_{11}) and a magnesium solid solution. Aluminum in the welding wire magnesium AZ61 enhances the wettability of a Mg-rich weld metal on Zn-coated steel sheet.

3. The strength of CMT welding-brazing Mg AZ31 to galvanized mild steel is determined primarily by the strength of the brazing interface.

4. The strength of the CMT welding-brazing lap-shear 1-mm-thick Mg AZ31-galvanized mild steel joint is comparable to the strength of lap-shear 1-mm-thick Mg AZ31-Mg AZ31 welded joint.

Acknowledgments

This work was financially supported by the National Nature Science Foundation of China (No. 51265028), and GM Research and Development Center, Warren, Mich.

References

1. Liu, L. M., and Zhao, X. 2008. Study on the weld joint of Mg alloy and steel by laser-GTA hybrid welding. *Material Characterization* 59: 1279–1284.

2. Yang, X. 2006. CMT: Cold Metal Transfer MIG/MAG dip-transfer process for auto-

Table 8 — Analysis of Variance for Tensile Strength Using SS (Sum of Square) for Tests

Source	SS (Sum of Square)	DOF	Variance	F	F (Critical)	Contribution (%)
A	15.5	3	5.2	0.276	6.590	15.14
B	17.125	3	5.7	0.306	6.590	16.73
C	7.4	3	2.5	0.132	6.590	7.23
D	17.74	3	5.91	0.317	6.590	17.33
E	20.933	3	6.98	0.374	6.590	20.45
A×B	4.176	3	1.39	0.075	6.590	4.08
A×C	1.7	3	0.57	0.030	6.590	1.66
C×D	1.316	3	0.44	0.024	6.590	1.29
Error	16.88	4	—	—	—	16.49
Total	102.35	31	—	—	—	100

Table 9 — Welding Variables and Tensile Load of Optimized Mg-Steel Weld Joint

Specimen No.	Welding Speed (mm/s)	Voltage (V)	Current (A)	Deviation Distance (mm)	Wire Feed Speed (m/min)	Load (kN)
9	7	10	55	2	5	5.5

Table 10 — EPMA Analysis Results of Various Zones Shown in Fig. 10

Regions in Fig. 10	Atomic Content in Percentage (at.-%) O	Fe	Mg	Al	Zn
1	4.44	0	93.00	0	4.44
2	65.23	0	25.81	5.69	1.24
3	2.90	0	54.38	36.22	6.50
4	4.41	0	90.09	1.51	1.65
5	65.23	0	25.81	5.69	0
6	2.30	0	63.03	29.26	5.41
7	6.35	3.90	23.11	11.49	51.32

mated applications. Arc welding machine 36(6): 5–7.

3. Zhang, H. T., Feng, J. C., Heb, P., Zhang, B. B., Chen, J. M., and Wang, L. 2009. The arc characteristics and metal transfer behavior of cold metal transfer and its use in joining aluminum to zinc-coated steel. *Materials Science and Engineering A* 499: 111–113.

4. Achar, D. R. G., Ruge, J., and Sundaresan, S. 1980. Verbinden von aluminum mit stahl, besonders durch schweiben (Joining of aluminum to steel, especially by welding). *Alumnium* 56(2): 174–193 (in German).

5. Achar, D. R. G., Ruge, J., and Sundaresan, S. 1980. Metallurgical and mechanical investigations of aluminum-steel fusion welds. *Aluminum* 56(6): 391–397.

6. Vollertsen, F., and Thomy, C. 2011. Laser-MIG hybrid welding of aluminum to steel — A straightforward analytical model for wetting length. *Welding in the World* 55(01-02): 58–66.

7. Davies, G. 2003. *Magnesium, Materials for Automotive Bodies*. Elsevier, G.: London, UK. pp. 91, 158, 159.

8. Blawert, C., Hort, N., and Kainer, K. V. 2004. Automotive applications of magnesium and its alloys. *Trans. Indian. Inst. Met.* 57(4): 397–408.

9. Aghion, E., and Bronfin, B. 2000. Magnesium alloys development towards the 21(st) centuries. Magnesium alloys. *Material Science Forum* 350(3): 19–28.

10. Gray, J. E., and Luan, B. 2002. Protective coating on magnesium and its alloys — A critical review. *J. Alloys Compd.* 336: 88–113.

11. Wu, C. S., Zhang, Z., and Cao, F. H. 2007. Study on the anodizing of AZ31 magnesium alloys in alkaline borate solution. *Appl. Surf. Sci.* 253: 3893-8.

12. Alvarez-Lopez, M., Pereda, M. D., and del Valle, J. A. 2010. Corrosion behavior of AZ31 magnesium alloy with different grain sizes in simulated biological fluids. *Acta Biomaterial* 6: 1763–1771.

13. Liu, C., Zhu, X., and Zhou, H. 2006. *Phase Diagram of Mg Alloys*. Central South University Press, Hunan, China.

14. Guo, Q., Wang, G., and Guo, G. 2009. *Binary alloy phase diagram of nonferrous metal.* Chemical Industry Press, Beijing, China.

15. Liu, L., and Qi, X. 2010. Strengthening effect of nickel and copper interlayers on hybrid laser-TIG welded joints between magnesium alloy and mild steel. *Materials and Design* 31: 3960–3963.

16. Qi, X., and Song, G. 2010. Interfacial structure of the joints between magnesium alloy and mild steel with nickel as interlayer by hybrid laser-TIG welding. *Materials and Design* 31: 605–609.

17. Watanabe, T., Kagiya, K., Yanagisawa, A., and Tanabe, H. 2006. Solid state welding of steel and magnesium alloy using a rotating pin. *Quart. Journal of Japanese Welding Society* 24: 108–123.

18. Chen, Y. C., and Nakata, K. 2009. Effect of tool geometry on microstructure and mechanical properties of friction stir lap welded magnesium alloy and steel. *Material Design* 30: 3913–3919.

19. Jana, S., Hovanski, Y., and Grant, G. J. 2010. Friction stir lap welding of magnesium alloy to steel: A preliminary investigation. *Metallurgical and Materials Transactions* 41A: 3172–3182.

20. Wei, Y., Li, J., and Xiong, J., et al. 2012. Microstructures and mechanical properties of magnesium alloy and stainless steel weld joint made by friction stir lap welding. *Materials and Design* 33: 111–114.

21. Roy, R. 1990. *Designs with Interactions, A Primer on Taguchi Method*. Van Nostrand Reinhold: New York, N.Y. p. 61.

22. Zhang, S. MATLAB 7.0 practical tutorial, China Machine Press, 2006.7.

23. Song, G., and Wang, P. 2011. Pulsed MIG welding of AZ31B magnesium alloy. *Materials Science and Technology* 27(2): 518–524.

24. Song, G., Wang, P., and Liu, L. M. 2010. Study on AC-PMIG welding of AZ31B magnesium alloy. *Science and Technology of Welding and Joining* 15(3): 219–225.

25. Ueyama, T., and Nakata, K. 2004. Pulsed MIG welding of magnesium alloy. *Kei Kinzoku Yosetsu* 42: 203–213.

26. Zhang, H. T., Feng, J. C., He., P., Zhang, B. B., Chen, J. M., and Wang, L. 2009. The arc characteristics and metal transfer behavior of cold metal transfer and its use in joining aluminum to zinc-coated steel. *Materials Science and Engineering A* 499: 111–113.

27. Cao, R., Yu, G., Chen, J. H., and Wang., P.-C. 2013. Cold metal transfer joining aluminum alloys to galvanized mild steel. *J. Mater. Process Technol*., in press.

28. Casalino, G., Curcio, F., Memolo, F., and Minutolo, C. 2005. Investigation on Ti6A14V laser welding using statistical and Taguchi approaches. *J. Mater. Process Technol.* 167: 422–428.